PROCEEDINGS OF SPIE

SPIEDigitalLibrary.org/conference-proceedings-of-spie

Kernel principle component analysis applied to Raman spectra to differentiate drugs administered to rabbit cornea in blind study

O'Connor, Sean, Gil, Eddie, Keppler, Mark, Scully, Marlan, Yakovlev, Vladislav

Sean P. O'Connor, Eddie M. Gil, Mark A. Keppler, Marlan O. Scully, Vladislav V. Yakovlev, "Kernel principle component analysis applied to Raman spectra to differentiate drugs administered to rabbit cornea in blind study," Proc. SPIE 11219, Visualizing and Quantifying Drug Distribution in Tissue IV, 1121907 (19 February 2020); doi: 10.1117/12.2546431



Event: SPIE BiOS, 2020, San Francisco, California, United States

Kernel principle component analysis applied to Raman spectra to differentiate drugs administered to rabbit cornea in blind study

Sean P. O'Connor*a, Eddie M. Gil^{b,c}, Mark A. Keppler^{b,c}, Marlan O. Scully^{a,d}, Vladislav V. Yakovlev^{a,b}

^aDepartment of Physics and Astronomy, Texas A&M University, College Station, TX 77843
^bDepartment of Biomedical Engineering, Texas A&M University, College Station, TX 77843
^cSAIC Corporation, JBSA Fort Sam Houston, TX 78234
^dDepartment of Physics, Baylor University, Waco, TX 76798

ABSTRACT

Scanning confocal Raman spectroscopy was applied for detecting and identifying topically applied ocular pharmaceuticals on rabbit corneal tissue. Raman spectra for Cyclosporin A, Difluprednate, and Dorzolamide were acquired together with Raman spectra from rabbit corneas with an unknown amount of applied drug. Kernel principle component analysis (KPCA) was then used to explore a transform that can describe the acquired set of Raman spectra. Using this transform, we observe some spectral similarity between cornea spectra and Cyclosporin A, with little similarity to Dorzolamide and Difluprednate. Further investigation is needed to identify why these differences occur.

Keywords: Chemical sensing, Cornea, Drug detection, Eye, Kernel principle component analysis, Ocular tissue, Raman imaging, Raman spectroscopy

1. INTRODUCTION

Detecting the distribution of ocular drugs in a spatially resolved regime provides many challenges, and evaluating the efficacy of drug application is important for optimizing drug delivery in tissue. To address this, Raman spectroscopy provides a chemical specific technique which is capable of assessing the chemical content of the tissue under study repeatably and non-invasively. This is crucial to pharmaceutical development and quality control. Previous studies attempting to quantify drug concentrations in the cornea have dealt with background fluorescence using peak ratios in their processing chain,^{2,3} or by differencing spectra acquired before and after application of drug to the sample.^{4,5} Recent techniques to remove background fluorescence involve approximation of the overall trend of the signal while minimizing the amount of subtraction during peaks.^{6,7} Alternatively, coherent Raman spectroscopy can be used to suppress fluorescence background and boost Raman signal strength.^{8,9} A simple way to deal with fluorescent background in spontaneous Raman spectroscopy is to use an averaging filter to perform the first approximation of the fluorescence spectrum, then subtracting this approximation from the original signal. Such an approach should provide us with a robust way of dealing with weak Raman signatures of chemicals present in a drug distribute in a large tissue volume. In this work, we conducted a blind study to determine which drug, if any, was applied to cornea samples. This first requires that we are able to quantify the difference between the cornea and drug Raman spectra. To do this, we acquired spectra of Dorzolamide, Difluprednate, and Cyclosporin A (the three drugs in question), and we acquired Raman spectra from 6 rabbit corneas at various points in the lateral direction and depths. Through those measurements, we identified spectral Raman bands of interest in the samples and perform background subtraction and standardization on each of the spectra. We use kernel principle component analysis (KPCA) to reduce the Raman spectra to 5 components. These components were used to visualize where each spectrum lies in relation to the others using a 5x5 scatter matrix. From our results it became apparent that there is enough dissimilarity between Dorzolamide, Difluprednate, and the corneas to infer that those 2 drugs at least were not present in substantial quantities in the investigated tissue samples. Cyclosporin A, however, may be present in small amounts. However, in order to improve the accuracy of such assessment, further investigations are needed in order to understand why and how these spectral maps represent the chemical composition of the samples.

*sean oconnor@tamu.edu

Visualizing and Quantifying Drug Distribution in Tissue IV, edited by Kin Foong Chan, Conor L. Evans, Proc. of SPIE Vol. 11219, 1121907 · © 2020 SPIE CCC code: 1605-7422/20/\$21 · doi: 10.1117/12.2546431

2. MATERIALS & METHODS

2.1 Drug Information

Three commonly used ophthalmological drugs were employed in the study. Difluprednate $(C_{27}H_{34}F_2O_7: 6\alpha, 9\alpha$ -Difluoroprednisolone 21-acetate 17-butyrate) and Cyclosporin A $(C_{62}H_{111}N_{11}O_{12})$ were purchased from Sigma Aldrich. Dorzolamide Hydrochloride $(C_{10}H_{16}N_2O_4S_3\bullet HCl)$ was purchased from Cayman Chemical. In preparation of those substances for Raman measurements, the drugs were deposited onto aluminum covered microscope slides with the shiny side of the aluminum foil facing towards the drug. Glass, which is normally utilized in microscope slides, displays a strong, broad fluorescence band at ~1380 cm⁻¹, ¹⁰ and recent work has shown that a layer of aluminum foil is an effective method to avoid glass fluorescence from microscope slides in Raman studies. ¹¹

2.2 Cornea Preparation

Young rabbit corneas were purchased from Pel-Freez Biologicals by our collaborators. Some of the corneal samples had the ocular drugs applied to them from the aforementioned list. Then, the corneas were transferred to our lab with the information of the drugs administered withheld for a blind study. The corneas were stored frozen at -20°C until the time of experiments, and individual cornea were brought up to room temperature prior to data collection. In preparation for testing, corneas were fixed onto the aluminum covered microscope slides with the shiny side facing towards the sample.

2.3 Confocal Raman Microscope

Raman spectra were acquired using a commercially available confocal Raman microscope (LabRAM HR Evolution, Horiba). The microscope is coupled to a 532 nm continuous wave laser (Ventus 532, Laser Quantum) with a maximum power output of 110 mW. During experiments, the power was attenuated to 25 mW or less to avoid potential damage to the cornea samples. Prior measurements of temperature distribution upon laser excitation, ^{12,13} which were performed for biological samples of similar chemical composition, indicate that we shouldn't expect any dramatic alterations to our samples at the power levels used in this study. A 10x objective (N.A. = 0.25, Olympus) was used to focus the laser onto samples, and the scattered light was collected through the same objective in a backscattering geometry. The collected light was dispersed by a grating with groove density choices of either 600 gr/mm or 1800 gr/mm. The 600 gr/mm grating was used during the duration of data collection since the spectral detection range is larger than the 1800 gr/mm grating and the spectral resolution remained sufficient enough to resolve peaks in the spectra and to distinguish unique features between different drugs. The dispersed spectra were recorded with an EMCCD coupled to the spectrometer.

2.4 Raman Spectra Acquisition

In the initial phase of the project, Raman spectra of Cyclosporin A, Difluprednate, and Dorzolamide were acquired from -100 cm^{-1} to 4000 cm^{-1} using 4573 bins. For each drug, six sample spectra were collected. Figure 1 shows the presence of characteristic Raman peaks between $400 - 1700 \text{ cm}^{-1}$, and $2500 - 3500 \text{ cm}^{-1}$. Raman spectra from the rabbit corneas were collected in those spectral ranges using 1253 bins for the high range, while 1284 bins for the low range. For each cornea an overall sample spectrum was acquired by scanning a 5x5x11 volumetric grid for a total of 275 spectra. Taking the z-direction perpendicular to the corneal surface, 1 mm step sizes were taken in the xy-plane, and $40 \text{ }\mu\text{m}$ step sizes were taken in the z-direction to cover the entire depth of the cornea. This process yielded 1429 usable cornea spectra (6 corneas). To increase the number of drug samples to be comparable to the number of cornea samples, the 6 drug spectra were duplicated with additional gaussian noise (mean = 0, standard deviation = 1). The spectra were also randomly shifted to the left or right by 0 to 5 bins. In this way, 1428 spectra were simulated in addition to the 6 samples collected.

2.5 Spectra Processing

Each spectrum was median filtered using a 9-point window to remove shot noise. The rabbit cornea samples contained a large upward trend in the 400 - 1700 cm⁻¹ range. Slight trends were also apparent in the 2500 - 3500 cm⁻¹ range. The spectra can be seen in Figure 2. These trends were removed by using a moving average filter with a window size of 90 bins. The resulting signal was subtracted from the original signal so that only the peaks remained. This method of detrending was applied to the drug spectra and the cornea spectra in both ranges for consistency.

2.6 Finding Clusters in Spectra

Once the spectra were median filtered and detrended, KPCA was performed to prepare the samples for visualization. This technique is a variant of principle component analysis (PCA), where a nonlinear kernel is applied to the product of the weights and their inputs, prior to solving. In this case a sigmoid kernel was used. This was done using scikit-learn's

implementation of KPCA. 15,16 The implementation parameters were set to 5 components, spread of 5 computing jobs. The maximum iteration was left as default.

3. RESULTS & DISCUSSION

The drug spectra had peaks of interest in the 400 - 1700 cm⁻¹ range and in 2500 - 3500 cm⁻¹ range. While there is some overlap in peaks in the upper-frequency spectral range for Difluprednate and Dorzolamide, the specific peaks are different enough to distinguish the drugs from manual observation. In the low-frequency spectral range the peaks are more distinct for each of the 3 drugs. This can be seen in Figure 1.

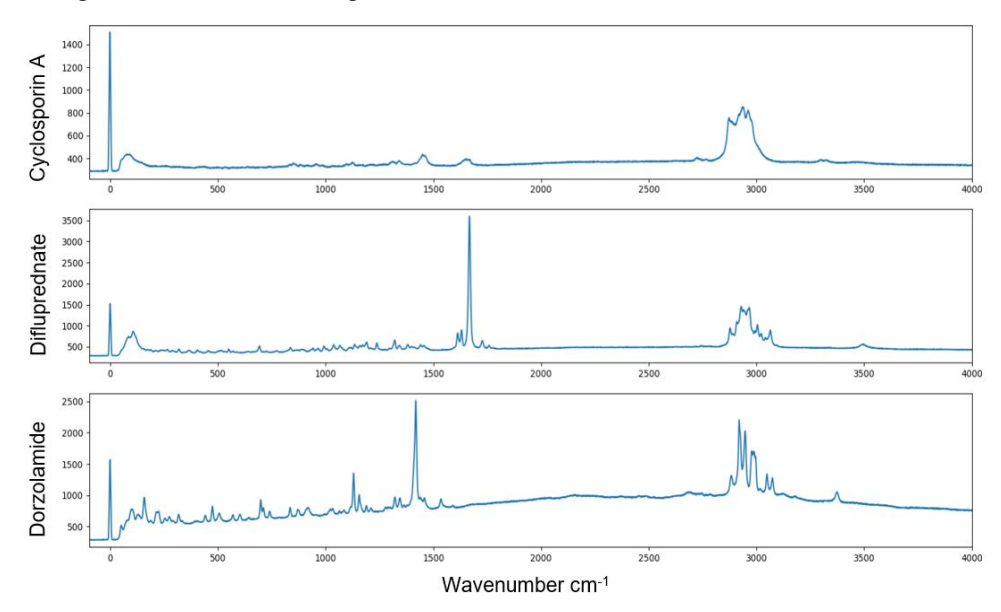


Fig. 1. Raman spectra for Cyclosporin A, Difluprednate, and Dorzolamide. The spectral range is from -100 to 4000 cm⁻¹.

Strong trends, which are indicative of a significant fluorescent background, were apparent in the rabbit cornea spectra as shown in Figure 2. Results of detrend on the peaks are shown. There is some hooking artifact near the end of a group of peaks. This is apparent near 3200 cm⁻¹ in the detrended rabbit cornea spectrum in Figure 2.

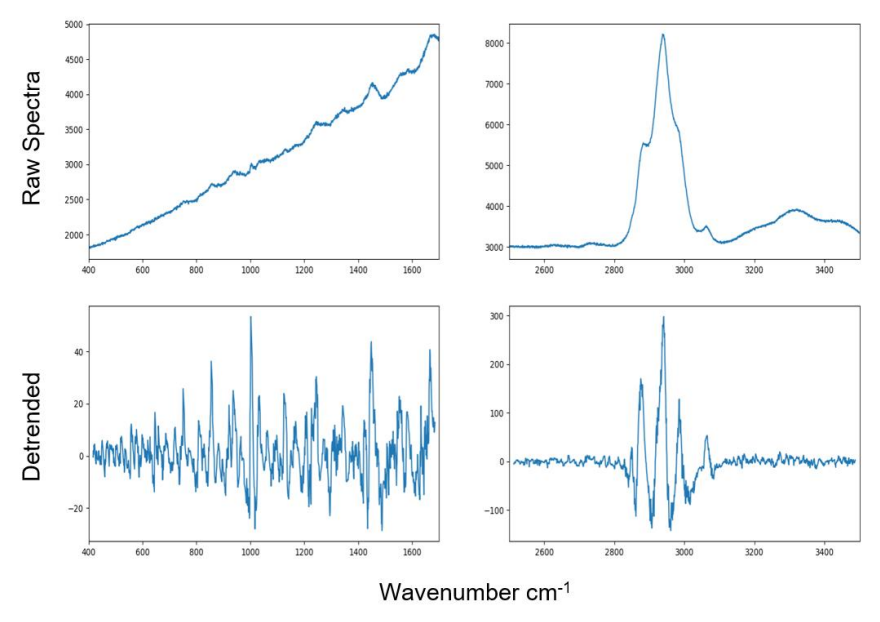


Fig. 2. Raman spectra for a cornea sample before and after the detrend procedure.

The detrend procedure was applied to all spectra in order to keep comparisons consistent. Detrended examples of the drug spectra and the cornea for both the low and upper ranges are shown in Figure 3. Again, there is some artifact near the edge of groups of Raman spectra.

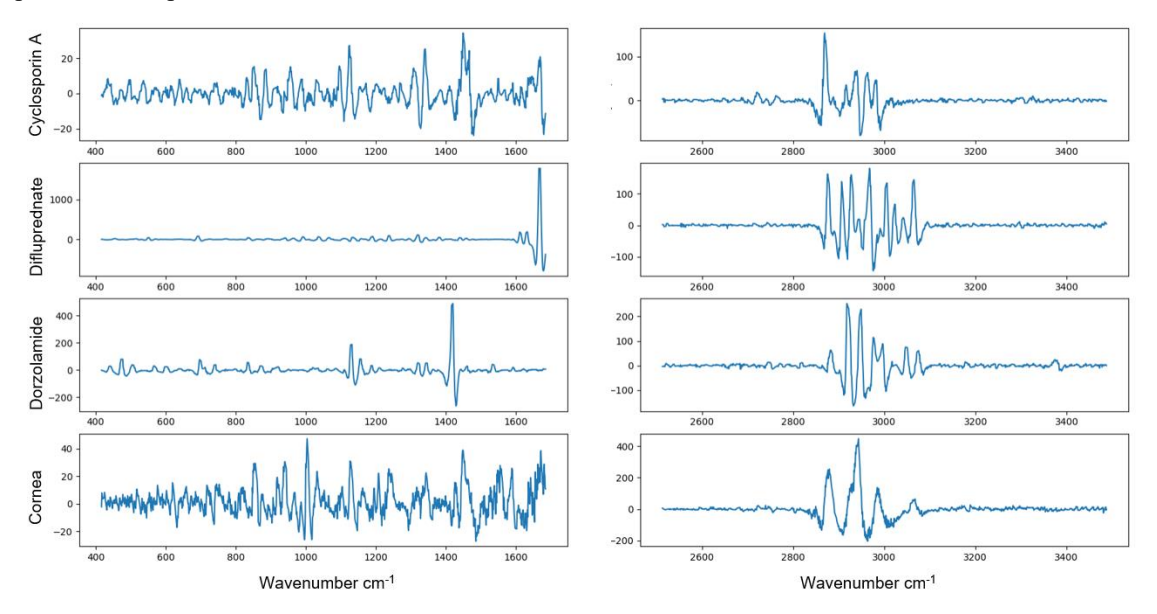


Fig. 3. Detrended Raman spectra for drug samples shown alongside cornea samples.

Kernel PCA was used to visualize the relative similarity of the corneas to the drug samples. A scatter matrix summarizing the results of the kernel PCA is shown in Figure 4. On the diagonal is the histogram for each of the components found. Each off-axis plot is a scatter plot of any given pair of features. In row 0 column 1, the x coordinates are feature 1, and the y coordinates are feature 0. Cyclosporin A, Difluprednate, and Dorzolamide are represented by blue, orange, and green dots respectively. All other points are samples taken from each of the corneas.

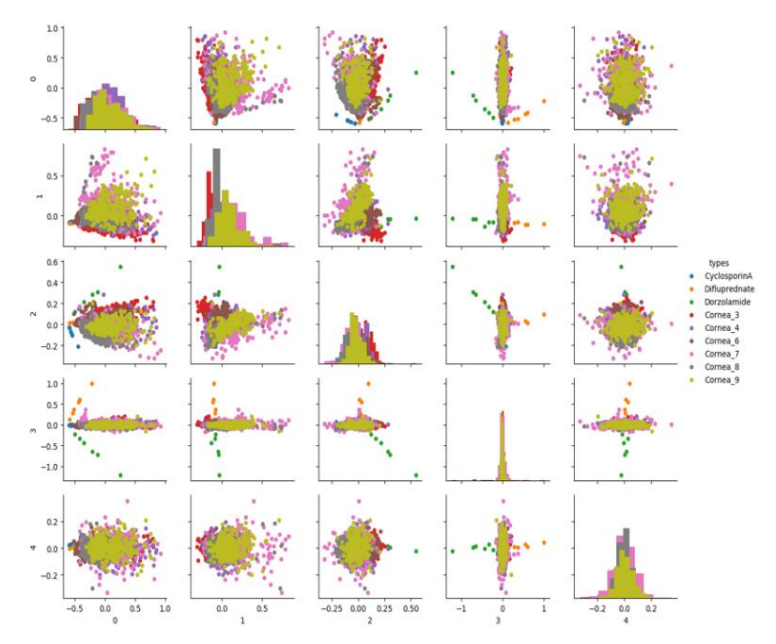


Fig. 4. Result of KPCA on samples in the 2500 – 3500 cm⁻¹ spectral range. Cyclosporin A, Difluprednate, and Dorzolamide are represented by blue, orange, and green dots, respectively. All other points are samples taken from each of the corneas.

The overall distance between clusters in each plot gives a qualitative description of general similarity between groups. This does not however, explain why that similarity exists. Figures 5 and 6 follow the same rule and color scheme. Figure

4 suggests that some features that resulted from this technique cluster Dorzolamide, and Difluprednate. The cornea samples cluster well with each other, while Cyclosporin A seemed to cluster near the corneas. The result of kernel PCA after increasing the number of drug samples with noisy and shifted copies is shown in Figure 5. Dorzolamide and Difluprednate are still consistently clustered by this technique as in Figure 4. However, Cyclosporin A samples cluster further away from the cornea samples than before.

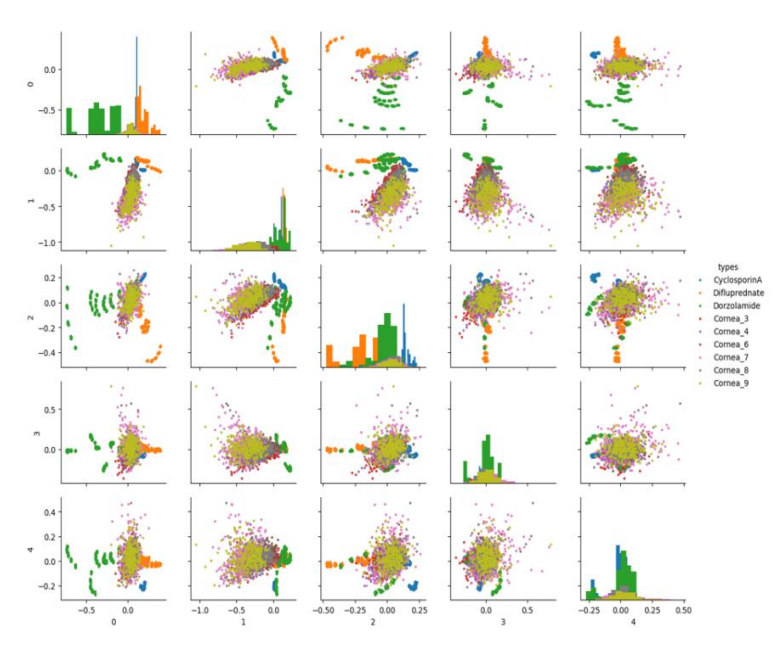


Fig. 5. Result of KPCA after up-sampling the number of drug samples. Cyclosporin A, Difluprednate, and Dorzolamide are represented by blue, orange, and green dots, respectively. All other points are samples taken from each of the corneas.

Concatenating the low range and high range of Raman spectra together offers a larger feature space to learn from. Thus, performing kernel PCA on the concatenated data could reveal alternative splits in the data. This is shown in Figure 6.

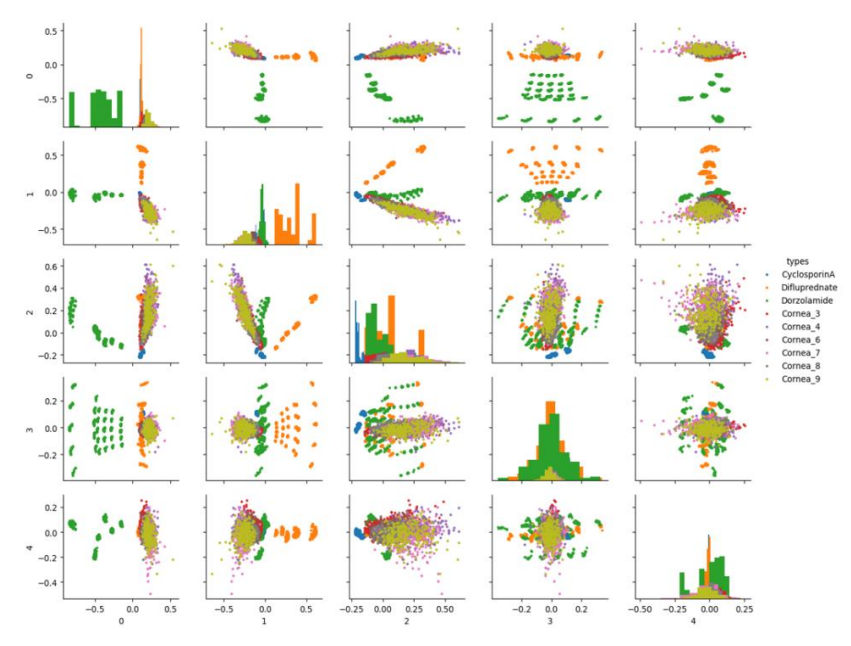


Fig. 6. Results of KPCA on concatenated spectra post up-sampling the number of drug samples. This allows the transform to learn from both the upper and lower ranges in the Raman spectra. Cyclosporin A, Difluprednate, and Dorzolamide are represented by blue, orange, and green dots, respectively. All other points are samples taken from each of the corneas.

Again, Difluprednate and Dorzolamide consistently form clusters, while Cyclosporin A cluster more closely with the cornea spectra. In each of the feature sets, there is some overlap of the drug samples with a small sub section of the cornea samples. More often than not, the drugs form clusters far from the rabbit corneas.

4. CONCLUSION

The procedure presented in this work shows that on the whole there is some similarity between the cornea spectra and the drug spectra. Since Dorzolamide and Difluprednate data consistently form distinct clusters located far from the cornea spectra, it is unlikely that those drugs were applied to the corneas. Cyclosporin A clustered close to the corneas. This technique only shows how similar each spectrum is on the whole. The technique does not show why these spectra cluster in the way they do. One source of this overlap could be from chemical bonds that corneal proteins have in common with each of the drugs. The approach described here is a way of assessing Raman spectra and analyzing small amounts of impurities with a strong tissue background. This strategy can be equally applied to analysis of coherent Raman spectra, ^{17,18} Brillouin spectroscopy and microscopy, ¹⁹⁻²¹ hyperspectral imaging and sensing, ^{22,23} and ultrasensitive detection of environmental pollutants. ^{24,25} In our future work, we intend to investigate algorithms for removing corneal reference spectra from the unknown corneas in order to leave behind only noise and peaks due to the presence of drugs if any.

ACKNOWLEDGEMENTS

S.P.O. is supported by the Herman F. Heep and Minnie Belle Heep Texas A&M University Endowed Fund held/administered by the Texas A&M Foundation. M.O.S. acknowledges support from the Office of Naval Research (N00014-16-1-3054) and the Robert A. Welch Foundation (Grant No. A-1261). V.V.Y. acknowledges partial funding from the National Science Foundation (NSF) (DBI-1455671, ECCS-1509268, CMMI-1826078), the Air Force Office of Scientific Research (AFOSR) (FA9550-15-1-0517, FA9550-18-1-0141), Army Research Laboratory (ARL) (W911NF-17-2-0144) the Office of Naval Research (ONR) (N00014-16-1-2578), the National Institutes of Health (NIH) (1R01GM127696-01), the Cancer Prevention and Research Institute of Texas (CPRIT) (RP180588). S.P.O. thanks Zhe He and Dr. Benjamin Strycker from Texas A&M University for helpful advice for operating the Raman microscope. The authors thank Dr. Srinath Palakurthi from Texas A&M Irma Lerma Rangel College of Pharmacy for providing the rabbit cornea samples.

REFERENCES

- [1] O'Connor, S. P., Lalonde, J., Nodurft, D. T. and Yakovlev, V. V., "(Re)defining sensitivity of chemical imaging," Vis. Quantifying Drug Distrib. Tissue III(March), C. L. Evans and K. F. Chan, Eds., 16, SPIE (2019).
- [2] Bauer, N. J., Wicksted, J. P., Jongsma, F. H., March, W. F., Hendrikse, F. and Motamedi, M., "Noninvasive assessment of the hydration gradient across the cornea using confocal Raman spectroscopy.," Invest. Ophthalmol. Vis. Sci. 39(5), 831–835 (1998).
- [3] Bauer, N. J., Motamedi, M., Wicksted, J. P., March, W. F., Webers, C. A. and Hendrikse, F., "Non-invasive assessment of ocular pharmacokinetics using Confocal Raman Spectroscopy.," J. Ocul. Pharmacol. Ther. **15**(2), 123–134 (1999).
- [4] Hosseini, K., March, W., Jongsma, F. H. M., Hendrikse, F. and Motamedi, M., "Noninvasive Detection of Ganciclovir in Ocular Tissue by Raman Spectroscopy: Implication for Monitoring of Drug Release," J. Ocul. Pharmacol. Ther. **18**(3), 277–285 (2002).
- [5] Hosseini, K., Jongsma, F. H. M., Hendrikse, F. and Motamedi, M., "Non-invasive monitoring of commonly used intraocular drugs against endophthalmitis by raman spectroscopy," Lasers Surg. Med. **32**(4), 265–270 (2003).
- [6] Zhang, Z.-M., Chen, S. and Liang, Y.-Z., "Baseline correction using adaptive iteratively reweighted penalized least squares," Analyst **135**(5), 1138 (2010).
- [7] Liu, X., Zhang, Z., Liang, Y., Sousa, P. F. M., Yun, Y. and Yu, L., "Baseline correction of high resolution spectral profile data based on exponential smoothing," Chemom. Intell. Lab. Syst. **139**, 97–108 (2014).

- [8] Arora, R., Petrov, G. I. and Yakovlev, V. V., "Analytical capabilities of coherent anti-Stokes Raman scattering microspectroscopy," J. Mod. Opt. **55**(19–20), 3237–3254 (2008).
- [9] Arora, R., Petrov, G. I., Liu, J. and Yakovlev, V. V., "Improving sensitivity in nonlinear Raman microspectroscopy imaging and sensing," J. Biomed. Opt. **16**(2), 021114 (2011).
- [10] Kamemoto, L. E., Misra, A. K., Sharma, S. K., Goodman, M. T., Luk, H., Dykes, A. C. and Acosta, T., "Near-Infrared Micro-Raman Spectroscopy for in Vitro Detection of Cervical Cancer," Appl. Spectrosc. **64**(3), 255–261 (2010).
- [11] Cui, L., Butler, H. J., Martin-Hirsch, P. L. and Martin, F. L., "Aluminium foil as a potential substrate for ATR-FTIR, transflection FTIR or Raman spectrochemical analysis of biological specimens," Anal. Methods **8**(3), 481–487 (2016).
- [12] Bixler, J. N., Hokr, B. H., Denton, M. L., Noojin, G. D., Shingledecker, A. D., Beier, H. T., Thomas, R. J., Rockwell, B. A. and Yakovlev, V. V., "Assessment of tissue heating under tunable near-infrared radiation," J. Biomed. Opt. 19(7), 070501 (2014).
- [13] Bixler, J. N., Hokr, B. H., Oian, C. A., Noojin, G. D., Thomas, R. J. and Yakovlev, V. V., "Assessment of tissue heating under tunable laser radiation from 1100 nm to 1550 nm," 3–8 (2015).
- [14] Chan, T., Payor, S. and Holden, B. A., "Corneal thickness profiles in rabbits using an ultrasonic pachometer.," Invest. Ophthalmol. Vis. Sci. **24**(10), 1408–1410 (1983).
- [15] Bakir, G. H., Weston, J. and Schölkopf, B., "Learning to find pre-images," Adv. Neural Inf. Process. Syst.(iii) (2004).
- [16] Pedregosa, F., Varoquaux, G., Gramfort, A., Michel, V., Thirion, B., Grisel, O., Blondel, M., Prettenhofer, P., Weiss, R., Dubourg, V., Vanderplas, J., Passos, A., Cournapeau, D., Brucher, M., Perrot, M. and Duchesnay, E., "Scikit-learn: Machine Learning in Python," J. Mach. Learn. Res. 12, 2825–2830 (2011).
- [17] Arora, R., Petrov, G. I. and Yakovlev, V. V., "Hyperspectral coherent anti-Stokes Raman scattering microscopy imaging through turbid medium," J. Biomed. Opt. **16**(2), 021116 (2011).
- [18] Arora, R., Petrov, G. I., Yakovlev, V. V. and Scully, M. O., "Chemical Analysis of Molecular Species through Turbid Medium," Anal. Chem. **86**(3), 1445–1451 (2014).
- [19] Traverso, A. J., Thompson, J. V., Steelman, Z. A., Meng, Z., Scully, M. O. and Yakovlev, V. V., "Dual Raman-Brillouin Microscope for Chemical and Mechanical Characterization and Imaging," Anal. Chem. **87**(15), 7519–7523 (2015).
- [20] Meng, Z., Bustamante Lopez, S. C., Meissner, K. E. and Yakovlev, V. V., "Subcellular measurements of mechanical and chemical properties using dual Raman-Brillouin microspectroscopy," J. Biophotonics 9(3), 201–207 (2016).
- [21] Meng, Z., Thakur, T., Chitrakar, C., Jaiswal, M. K., Gaharwar, A. K. and Yakovlev, V. V., "Assessment of Local Heterogeneity in Mechanical Properties of Nanostructured Hydrogel Networks," ACS Nano 11(8), 7690–7696 (2017).
- [22] Petrov, G. I., Doronin, A., Whelan, H. T., Meglinski, I. and Yakovlev, V. V., "Human tissue color as viewed in high dynamic range optical spectral transmission measurements," Biomed. Opt. Express **3**(9), 2154 (2012).
- [23] Cone, M. T., Mason, J. D., Figueroa, E., Hokr, B. H., Bixler, J. N., Castellanos, C. C., Noojin, G. D., Wigle, J. C., Rockwell, B. A., Yakovlev, V. V. and Fry, E. S., "Measuring the absorption coefficient of biological materials using integrating cavity ring-down spectroscopy," Optica 2(2), 162 (2015).
- [24] Bixler, J. N., Cone, M. T., Hokr, B. H., Mason, J. D., Figueroa, E., Fry, E. S., Yakovlev, V. V. and Scully, M. O., "Ultrasensitive detection of waste products in water using fluorescence emission cavity-enhanced spectroscopy," Proc. Natl. Acad. Sci. 111(20), 7208–7211 (2014).
- [25] Bixler, J. N., Winkler, C. A., Hokr, B. H., Mason, J. D. and Yakovlev, V. V., "Utilizing scattering to further enhance integrating cavity-enhanced spectroscopy," J. Mod. Opt. **63**(1), 76–79 (2016).